EVAPORATION FROM N-HEPTANE DROPS IN AN AIR STREAM

Thesis by

William Louis Burriss

In Partial Fulfillment of the Requirements

For the Degree of Chemical Engineer

California Institute of Technology

Pasadena, California

1954

Acknowledgment

Financial support for this research program has been supplied by the Fluor Corporation and the California Institute of Technology. Dr. B. H. Sage has supervised and planned the project. N. T. Hsu has diredted the laboratory work and is responsible for most of the data. R. Rinker and S. Rodriguiz assisted with the construction of the apparatus. The author wishes to express appreciation for the assistance of the members of the department staff in this project.

TABLE OF CONTENTS

LIST OF FIGURES

LIST OF TABLES

I ABSTRACT

The rates of heat and mass transfer from equilibrium non-spherical n-heptane drops in an air stream have been investigated. Two types of drops were produced, one wetting the supporting tube and another not wetting the supporting tube. The drops ranged from 0.005 to 0.008 ft in diameter. Measurements were made at bulk air velocities between 2 and 8 fps, with an air temperature of 100°F. A semi-empirical relation taking into account the deviation of drop shape from spherical leads to a satisfactory correlation of data with those obtained by other investigators for spherical drops.

II INTRODUCTION

Langmuir (1) investigated the rate of evaporation from small spheres of iodine and found that the time rate of change of surface area is constant. Fuchs (2) considered the evaporation of small spherical drops of a material with a vapor pressure low relative to the total pressure in a stationary gas atmosphere and extended the theory to include the cases of finite vapor pressure, lowering of the drop temperature due to evaporation, limited evaporation space, and the non-stationary process. Langmuir's results (1) were a special case in this treatment. Bradley, Evans, and Whytlaw-Gray (3) found that the behavior of small drops of dibutyl phthalate and butyl stearate followed the predictions of Fuchs (2) at low pressures.

There is a relatively small amount of information available concerning simultaneous heat and mass transfer from small, isolated droplets at finite air velocities. Much of the previous work has been with drops of a fluid of low volatility where the mass transfer process is predominant. Froessling (4) treated the evaporation of low-volatility drops in a moving fluid both theoretically and experimentally. He developed a relation giving the Nusselt number as a function of the Reynolds number and Prandtl number.

$$(1) \qquad Nu = A + B\,(Re)^{a}\,(Pr)^{b}$$

The dimensionless mass transfer group analogous to the Nusselt number (the Sherwood number) is given as a similar function of the Reynolds number and Schmidt number.

$$(2) \quad Sh = A + B\,(Re)^a (Sc)^b$$

The values for the constants in equations (1) and (2) vary somewhat, different investigators obtaining slightly different values.

The evaporation from drops has been considered in some detail from a theoretical standpoint. Four simultaneous, partial differential equations may be written to describe the processes involved (Appendix). A general solution of these equations has not been found at the present time. Solutions exist for a number of special cases. In general, the complexity of the resulting expressions has limited the utility of this approach. It is possible to demonstrate from these equations that at zero velocity,

$$(3) \quad Nu = Sh = 2.0$$

which is in agreement with the observations of many investigators.

Heat transfer from spheres has been investigated in some detail, both theoretically and experimentally. Johnstone (5) presented a solution for the Fourier—Poisson equation for heat transfer to spheres in a moving sluid, assuming irrotational flow and the existence of a velocity potential. The experimental values obtained by Johnstone (5) and others are somewhat lower than those predicted from the theory. The effect of turbulence on heat transfer from a relatively large sphere (0.5 inch diameter) has been investigated in some detail (6).

The most recent work involving simultaneous heat and mass transfer from spheres is that of Ingebo (7) and Ranz and Marshall (8). Ingebo studied equilibrium drops formed on a pith sphere. Fluid was injected into the sphere to maintain a wet surface. Drops of a number of different fluids were investigated and the heat transfer data obtained were correlated by the following relation:

$$(4) \qquad Nu = 2.0 + Re^{.60} Sc^{.60} \ (.303) \ (K_a/K_v)$$

The rate of evaporation from drops is determined from an energy balance for the drop, using equation (4).

Ranz and Marshall (8) were primarily interested in water drops and considered the effect of dissolved materials in some detail. The water drops were suspended on a thermocouple and liquid was added to the drop by means of a small glass tube in order to maintain the drop at constant size. Ranz and Marshall used the correlation of Froessling (4) with modified constants:

$$(5) \qquad Nu = 2.0 + .600 \ Re^{.50} Pr^{.33}$$

$$(6) \qquad Sh = 2.0 + .600 \ Re^{.50} Sc^{.33}$$

The evaporation of pure liquid drops involves heat transfer to the drop by conduction, convection and radiation. In addition, the energy associated with the material added and removed in evaporation must be included in the energy balance. A simplification of treatment results if the drop is maintained at constant size. Non-equilibrium mass transfer from hydrocarbon drops has been considered from a

theoretical standpoint (9).

Recent work has indicated the possibility of resistance to mass transfer at the surface of the drop (10). This may prove to be important in convective transfer, but experimental verification depends not only upon refinement in experimental techniques but also upon a more complete understanding of local behavior across the transfer path.

III APPARATUS

The apparatus was designed for the study of isolated, equilibrium drops in a controlled air stream. The drops were supported on small glass or steel tubes in the air stream. Liquid was passed through a feed line from the injector into the drop in order to maintain the drop at essentially constant size during the measurements. The liquid in the injector was displaced by a plunger that was driven through a gear train by a variable speed motor, the speed of which could be accurately controlled and measured.

The air was supplied by a centrifugal blower which brought air in from outside the building. The blower was equipped with a variable speed drive. A venturimeter was used to set air mass rates that corresponded to nominal bulk velocities based on average laboratory conditions of 2, 4, 6, and 8 feet per second at the test section. During the course of a run, the air mass rate was held constant to within 0.4%.

The temperature of the air was controlled by several fixed and adjustable electric heaters, as well as by a thyratron-supplied control heater which was actuated by means of a platinum resistance thermometer. In order to reduce temperature gradients in the air stream, adjustable heaters were wound on the outer surface of the air duct downstream of the air heaters. In addition, it was found that temperature gradients had developed in passing through the rather long duct from the blower to the drop apparatus. In order to compensate

for this, several heaters were provided that added varying amounts of heat to different parts of the air stream, as determined by a temperature traverse at the outlet section. These precautions were sufficient to reduce the temperature gradients in the air stream within a two-inch radius of the drop to less than 0.3 degree per inch. Air temperatures were measured with calibrated copper-constantan thermocouples.

Turning vanes were located in the two elbows of the air duct immediately upstream of the test section. Straightening vanes were placed ahead of the converging section. A velocity traverse of the air stream at the test section (converging section discharge) using a hot-wire anemometer showed the velocity profile was uniform across the channel within 5% up to 1/4 inch from the wall. The level of turbulence was found to be low with the root mean square of the fluctuating velocities amounting to 1.3% of the air bulk velocity.

The drop support tube was mounted on steel tubing having an airfoil section. The airfoil could be moved in three directions in the air stream by means of a traversing gear. Two additional fittings were provided on the airfoil for pitot-tube connections. Various sample tubes were used during the course of the work. Probably the most satisfactory was a glass tube (diameter approximately 0.01 inch) with a flare on the end formed by blowing a small sphere and grinding away most of it by careful hand lapping. A calibrated 1-mil, platinum-constantan thermocouple was used to measure drop temperature.

The portion of the injector containing the fluid was immersed in an agitated oil bath, the temperature of which was controlled

within 0.1°F. Particular care was taken in thermostating the feed line from the injector to the drop support tube since considerable difficulty had been experienced earlier from drift in the temperature of the fluid in the feed line. A heater was wound on a large tube which served as a thermostat for the smaller feed tube. Oil from the injector bath was circulated in the annulus between the tubes. A differential thermocouple located at the extremes of the line was used in the adjustment of the heater wound on the larger tube. These precautions were apparently adequate for reproducible data were obtained subsequently.

A variable-ratio gear box, located between the motor and injector, provided five reduction ratios from 1:1 to 1:625 in multiples of five. The speed of the injector drive motor could be controlled and measured to 0.1% over a range of almost 10 to 1 in speed. A detailed description of the motor control is to be found elsewhere (11) and only a brief description will be included here.

The time standard used in the motor speed control was a 100-kilocycle, crystal-controlled oscillator which has a precision not less than 0.02%. The 100-kilocycle frequency was divided by ten electronically, and a 10 kilocycle timing standard was supplied to the predetermined counter. The predetermined counter consisted of four decade scalers and would count any predetermined number of pulses from 1 to 9999, furnish an output pulse, clearing and resetting automatically. In this manner, timing pulses from around 1 per second to 10 per second could be obtained with a precision not less than 0.1%. These pulses were broadened and supplied to a servo amplifier that controlled the speed of the injector drive motor.

The shunt field of the direct-current compound-wound motor was supplied from a constant 110-volt-direct-current source. The armature current was supplied by a thyratron power supply which served to control the speed of the motor. A photocell was illuminated through a rotating spiral on a Lucite disk. The output voltage of the photocell varied as a function of the angular position of the disk. This voltage was supplied to an electronic clamp that was actuated by the previously mentioned timing pulses. The output of the clamp controlled the speed of the motor through the thyratron supply. In operation, the thyratron supply maintained the motor at essentially constant speed. With varying load, the disk received angular displacement so that more or less light fell on the photocell at the timing pulse and the power input to the motor was suitably adjusted, automatically. Like all such mechanisms, the error is reduced if a substantial portion of the power input is controlled manually. This reduces the range of automatic control, but greatly improves the sensitivity, essentially eliminating hunt. The motor can control perfectly at multiples of the desired speed. The operator can easily tell if this is happening, however, and take remedial action, that is, change the setting on the manual power control for the motor. A neon light that was actuated by the timing pulses illuminated markers on the Lucite disk enabling the operator to determine whether the motor was controlling properly or not.

Unlike most of the previous studies of evaporation from drops, the drops in this investigation deviated substantially from spheres. As a consequence, the photographic equipment is particularly important. The drops were photographed on fine-grain cut film with a lens extension that gave a magnification of 5 to 1 on the film. Additional magnification was secured in photographic enlargement of the data negatives and in comparator measurements of the drops from the negatives. A tube, the diameter of which was known to 0.3%, was photographed simultaneously with the drops thereby furnishing a convenient scale. An electronic flash unit was used as the light source for the photography since it has a very high peak intensity with extremely short duration (approximately 100 microseconds) thereby minimizing the effect of any motion of the drop and likewise minimizing heat transfer by radiation from the photographic light to the drop. Best results were obtained using transmitted rather than reflected light, since surface reflections were less troublesome and the light was more efficiently utilized.

IV EXPERIMENTAL PROCEDURE

The air supply and thermostats were started several hours before the actual measurements were to be made, in order for the apparatus and the room to approach thermal equilibrium. It was desired to maintain the room as near air supply temperature (100°F) as possible. The room temperature was usually approximately 97°F during the measurements. When the thermostats and air supply had been adjusted to the proper conditions, observation of the drops was commenced. The drop was observed through a telescope and when growth had apparently ceased, usually less than a minute after removal of the previous drop, the drop was photographed. At least three separate drops were photographed for each condition. The three drops contained on a single negative were all ordinarily made in a ten minute period. Additional measurements under presumably identical conditions were made on subsequent days, in order to verify the reproducibility of the data.

The experimental results are summarized in Table I. In some of the tests, the sample tube was coated with a material (perfluoro-octanoic acid) not wet by hydrocarbons. Figure 8 is an enlargement of a typical data negative obtained using this agent. This can be compared with a wetting drop shown in Figure 7. There is some doubt as to where the wetting drop ends which contributes somewhat to the uncertainty in the area measurements for these drops.

Drop surface areas and volumes were estimated by graphical integration of enlarged prints of the data negatives and by graphical

integration of plots made from comparator measurements of the negatives. Satisfactory agreement was found, although the latter technique is thought to be more accurate. The comparator measurements of the drops considered here have been published (12).

V RESULTS AND DISCUSSION

The Sherwood number was calculated from the following relation:

$$(7) \qquad Sh = \frac{6\ m\ P^2\ \alpha}{\rho_a\ D_v\ f_v}$$

This expression assumes mixtures of air and n-heptane to be ideal solutions. The fugacity of n-heptane was evaluated from the Benedict equation (12) and is accurate to 1% for the range of temperature of interest here. The other properties of n-heptane required in the calculations were obtained from Rossini (13). Substitution of partial pressures for fugacity results in the conventional expression for the Sherwood number. The assumption of perfect gas behavior is then involved.

The Reynolds number was based on free stream conditions and maximum drop diameter as given in the following equation:

$$(8) \qquad Re = \frac{D\ U}{\nu}$$

The properties of air were obtained from a recent revue of the literature (14). The Schmidt number was similarily based on free-stream conditions using the following approximate relation:

$$(9) \qquad Sc = \frac{P\ \nu}{D_v}$$

Derived data, including the Reynolds, Schmidt and Sherwood numbers are listed in Table II.

The drops investigated varied greatly in shape from oblate spheroids to distended pendant shapes. For a low level of turbulence, the Sherwood number was postulated to be a linear function of the sphericity

and the height-diameter ratio of the drop.

$$(10) \quad Sh = (2 + K_1 Re^{.50} Sc^{.33}) \left[1 - K_2(1 - \lambda)\right] \left[1 + K_3 \left|1 - \frac{H}{D}\right|\right]$$

Statistical methods were used to evaluate the constants, the following constants resulting in a standard error of estimate of 4.9%:

$$(11) \quad \begin{cases} K_1 = 0.544 \\ K_2 = 1.147 \\ K_3 = 0.371 \end{cases}$$

Equation (10) can be written to show the relationship between the rate of evaporation and the sphericity.

$$(12) \quad \frac{m}{m_{\lambda=1}} = \frac{Sh_e}{Sh_{\lambda=1}} = \frac{Sh_e}{(2 + .544 Re^{.50} Sc^{.33}) \left[1 - .371 \left|1 - \frac{H}{D}\right|\right]}$$

Figure 9 illustrates the effect of drop sphericity on the rate of evaporation.

Similarily, the following expression indicates the relation between the rate of evaporation and the height-diameter ratio:

$$(13) \quad \frac{m}{m_{H/D=1}} = \frac{Sh_e}{Sh_{H/D=1}} = \frac{Sh_e}{(2 + .544 Re^{.50} Sc^{.33}) \left[1 + 1.147 (1 - \lambda)\right]}$$

Figure 10 shows the effect of H/D on the rate of evaporation. Both Figure 9 and Figure 10 show increasing evaporation rates with increasing deviation of the drop shape from spherical.

The drop temperatures measured with the 1 mil platinum-constantan thermocouple range from 62°F to around 65°F, the lower temperatures being

obtained with the larger drops. A number of investigators have found the drop temperature to be equal to the wet bulb temperature for the given fluid, within the accuracy of their measurements. The correlation of Ingebo (7) between psychrometric data for water and various fluids leads to a calculated wet bulb temperature of 60.6°F for n-heptane. Approximate calculations using heat transfer coefficients of McAdams (16) indicate that the spread in measured drop temperature may be due to the conduction of heat to the junction in the drop. This is substantiated by the apparent temperature gradient measured in the drop. The asymmetrical gradient measured can be accounted for by the difference in thermal conductivity between platinum and constantan.

An energy balance can be written for drops that are maintained at constant size by equating the latent heat transfer with the sum of the heat transfer by convection, conduction, and radiation. The loss in latent heat is given by difference in enthalpy between the liquid and the vapor leaving the drop. Heat transfer by radiation is small in this case, representing approximately 1% of the total heat transfer. On the other hand, heat conduction in the drop support tube amounts to about 13% of the total, since the tubes used were large relative to the drop diameter. Additional data concerning the temperature gradient in the support tube are desirable in order to apply a suitable correction. In view of the uncertainty arising from this source, correlation of heat transfer data has not been undertaken.

Figure 11 is a plot of the mass transfer data, reduced to spheres by Equation 10, compared with the correlation of Froessling (4) and Ranz and Marshall (8) for spherical drops. The data fit equation (7) with

a standard deviation of 4.87% in Sherwood number. Use of different constants and a different exponent for the Reynolds number results in an improved fit for these data.

$$(14)\quad Sh = (2.0 + .356\ Re^{.56} Sc^{.33}) \left[1 + 2.292\ (1 - \lambda)\right] \left[1 - .257\ \left|1 - \frac{H}{D}\right|\right]$$

A standard deviation of 4.4% in Sherwood number was obtained using this relation for the data covered by this thesis (15).

VI CONCLUSIONS

The experimental data obtained with non-spherical n-heptane drops correlate with those obtained by other investigators for spherical drops when deviation from spherical shape is taken into account as given by the following expression:

$$(10) \quad Sh = (2 + .544Re^{.50}Sc^{.33}) \left[1 - 1.147(1 - \lambda)\right] \left[1 + .371 \left| 1 - \frac{H}{D} \right|\right]$$

The main source of error is probably in the determination of the surface area and volume of the drop. This uncertainty leads to a probable error of approximately 1% in Sherwood number. The average standard deviation in a group of data taken under similar conditions was less than 1% in Sherwood number. The precision of the data is believed to be substantially higher than the fit in the correlation used indicates (standard deviation of 4.9% for experimental data from equation (10)). The macroscopic nature of the basic correlation probably presents a limitation. An approach, preferable from the theoretical standpoint to use of the two given geometrical factors, consists of assigning relative weight to various areas of the drop in consequence of the varying effectiveness in evaporation. This can be approached by consideration of the boundary layer surrounding the drop. For example, it is reasonable to expect the leading edge of the drop to be most effective in material transfer since the laminar boundary layer is of minimum thickness at that point. Consideration of transfer effectiveness over the surface of the drop should ultimately permit more accurate prediction of evaporation from drops of varying geometry.

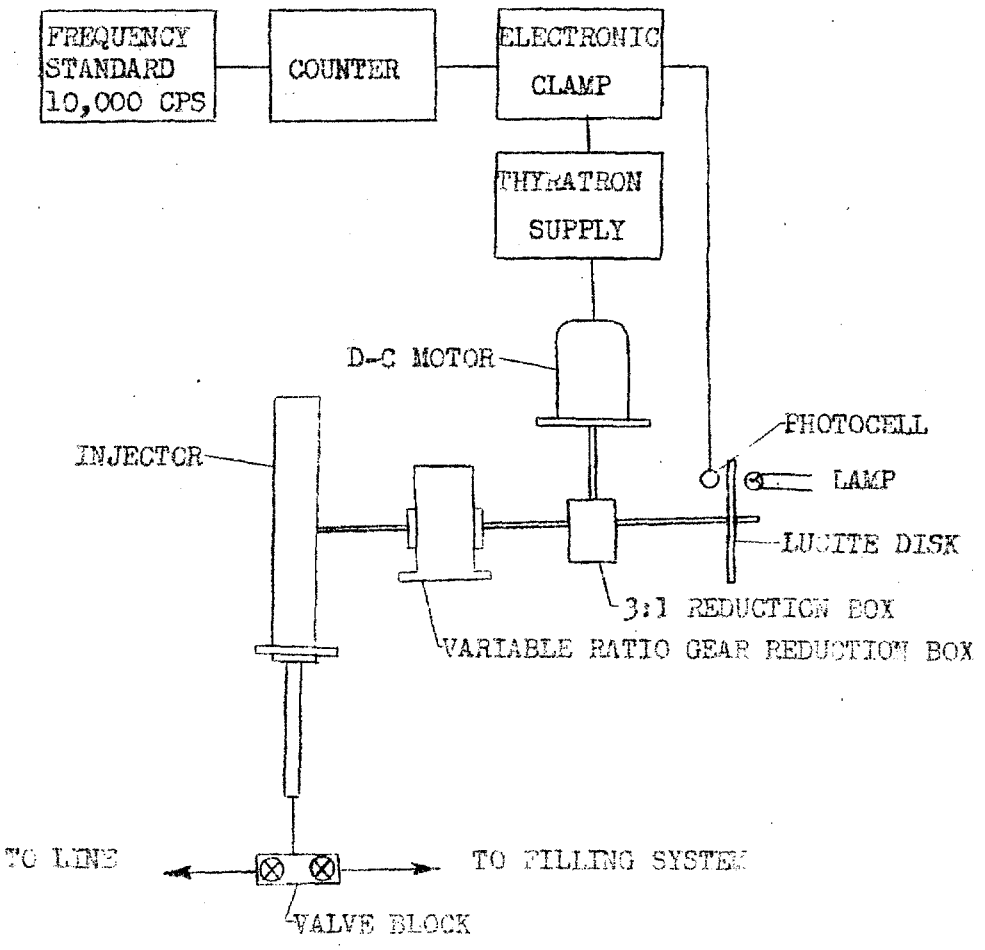

FIGURE 1 - SCHEMATIC OF INJECTOR DRIVE

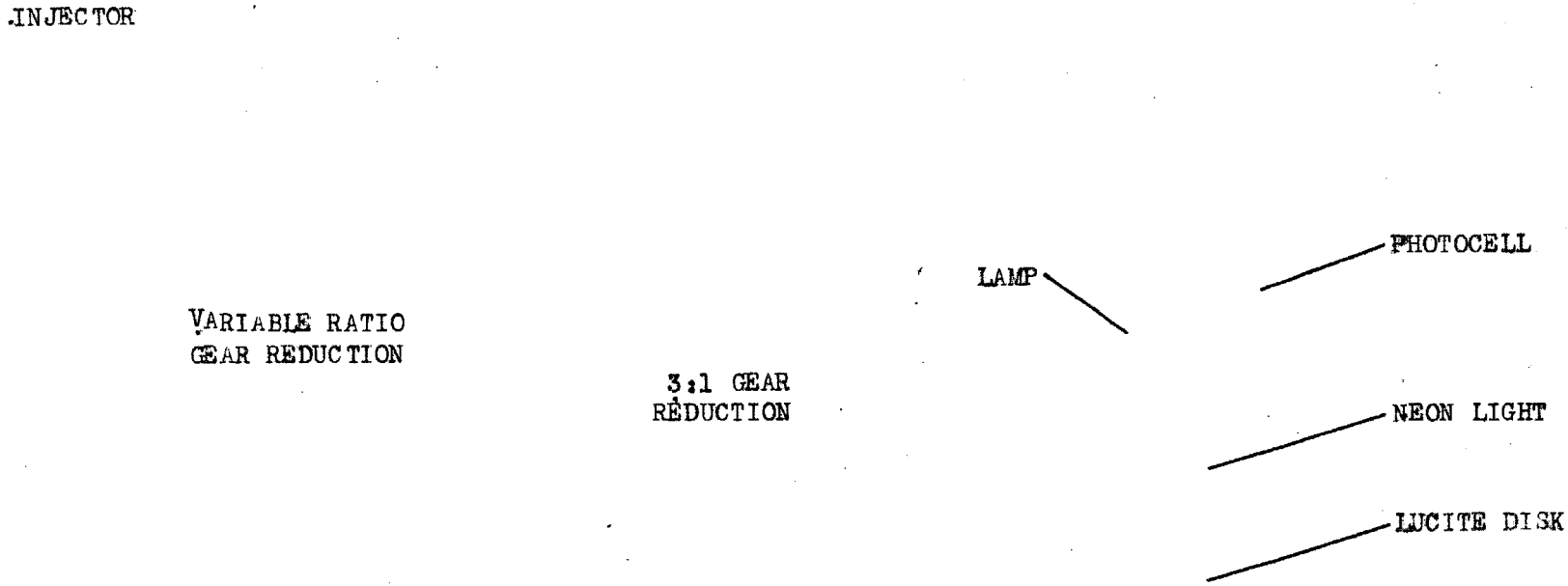

FIGURE 2 - INJECTOR DRIVE

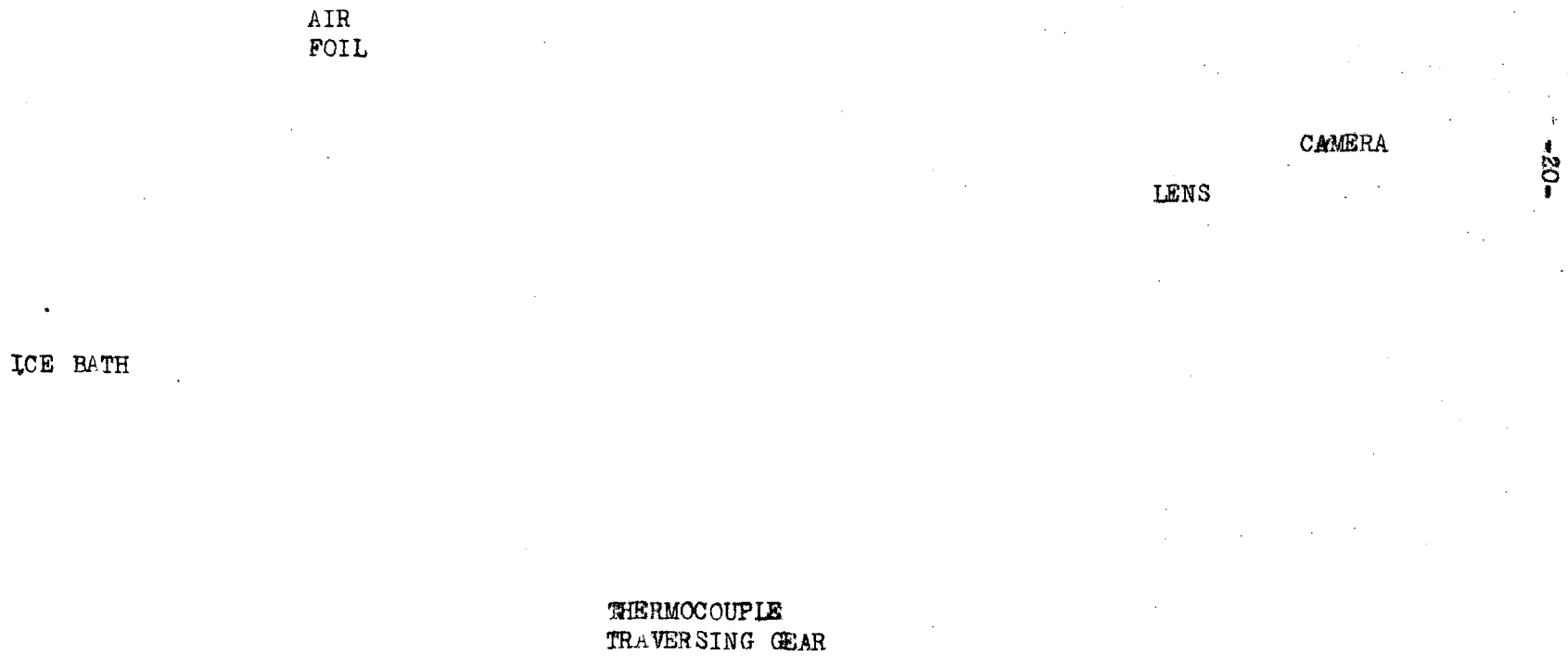

FIGURE 3 - DROP APPARATUS, TOP VIEW

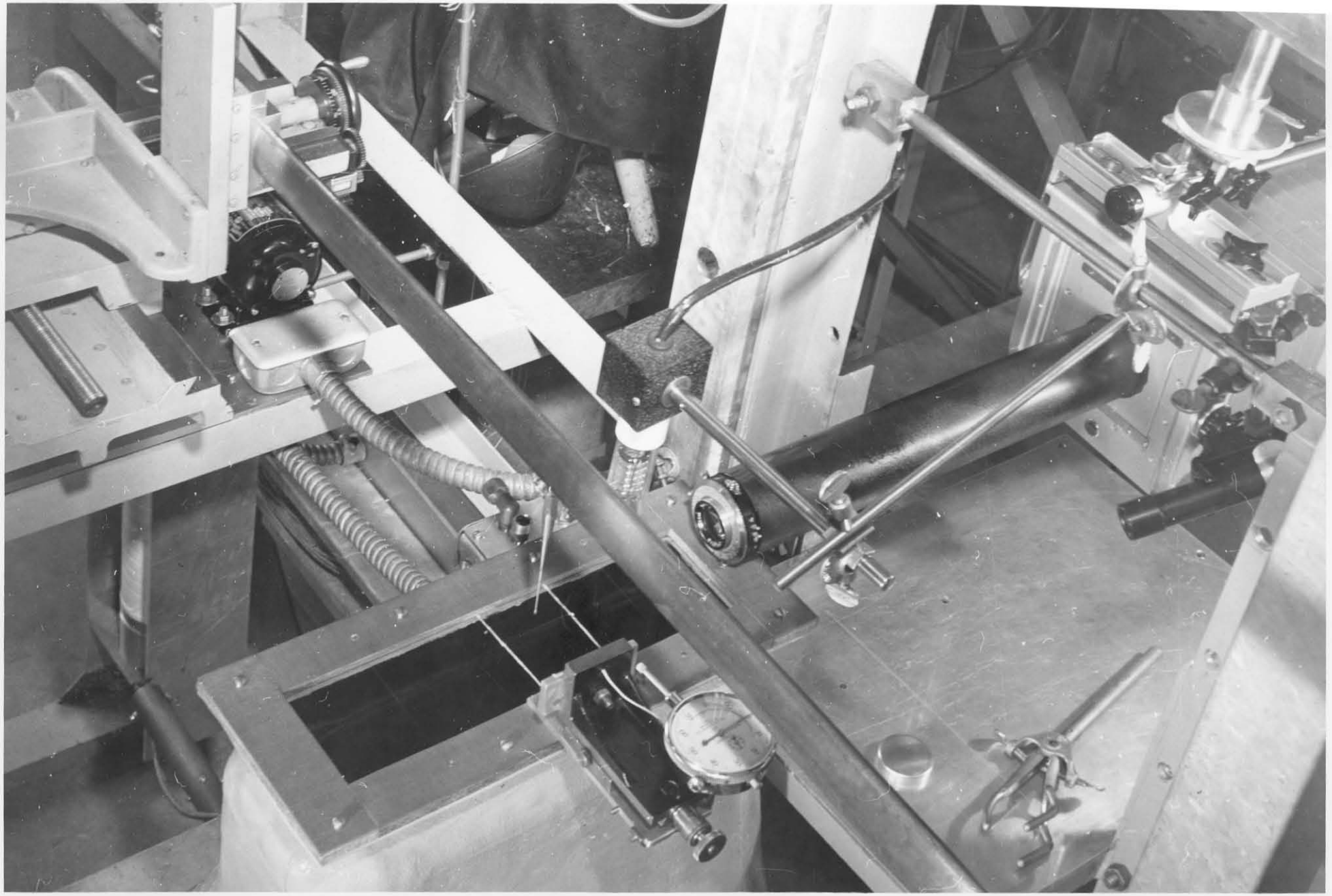

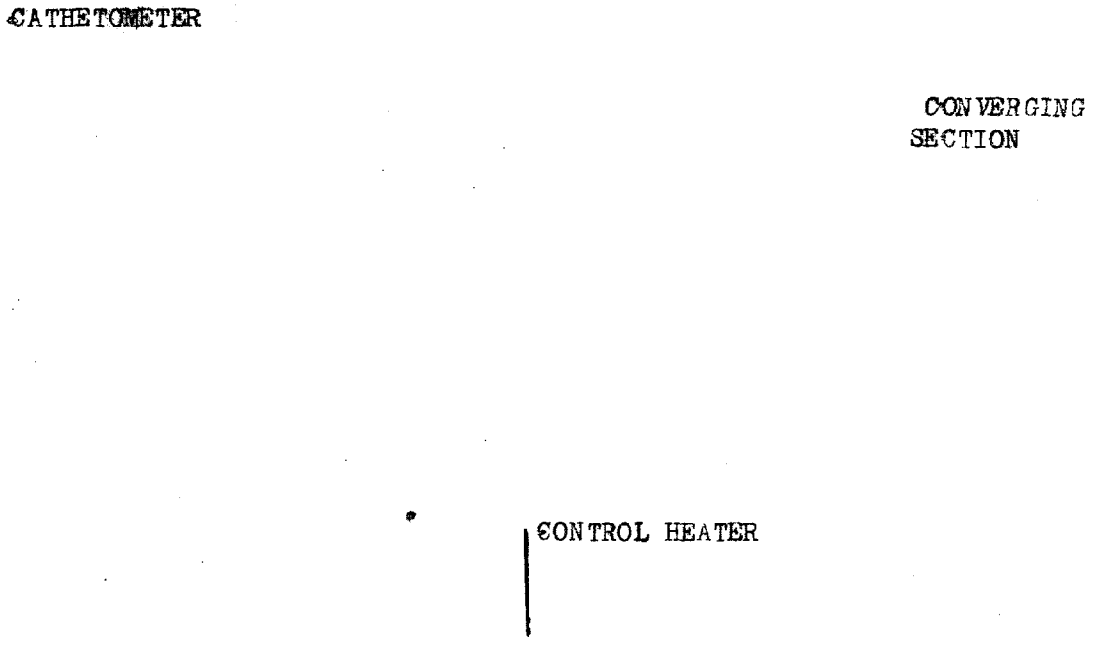

FIGURE 4 - DROP APPARATUS, SIDE VIEW

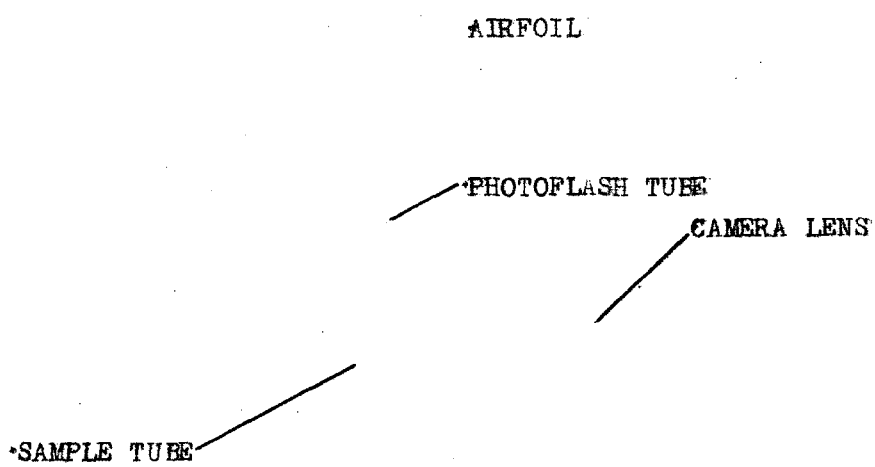

FIGURE 5 - DROP APPARATUS, SIDE VIEW

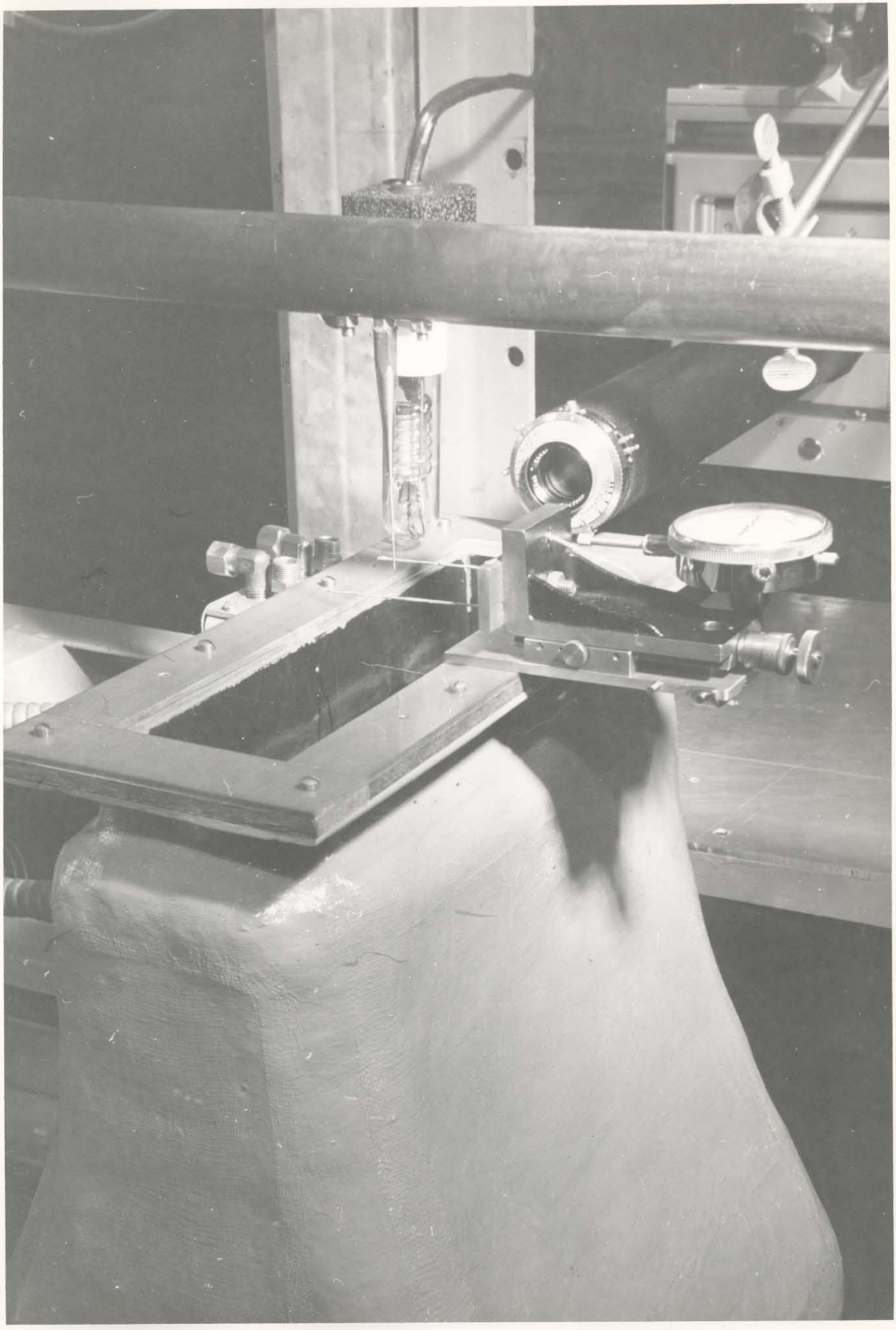

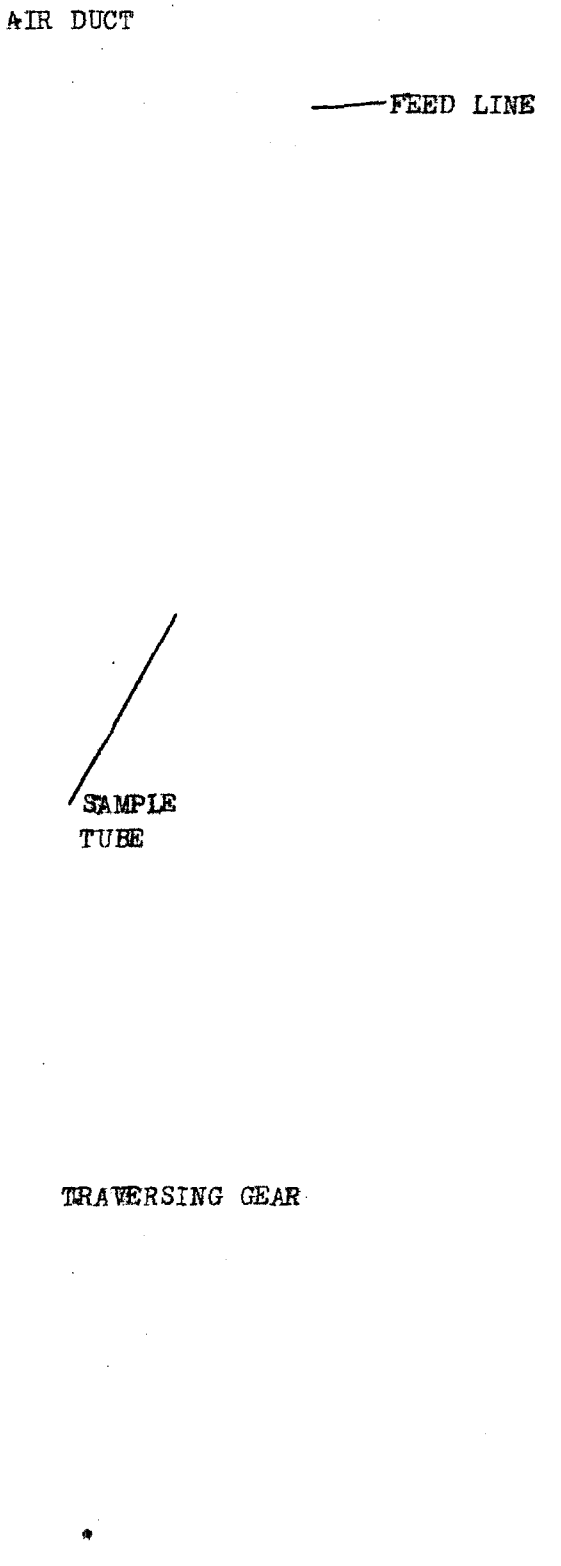

FIGURE 6 - DROP APPARATUS, REAR VIEW

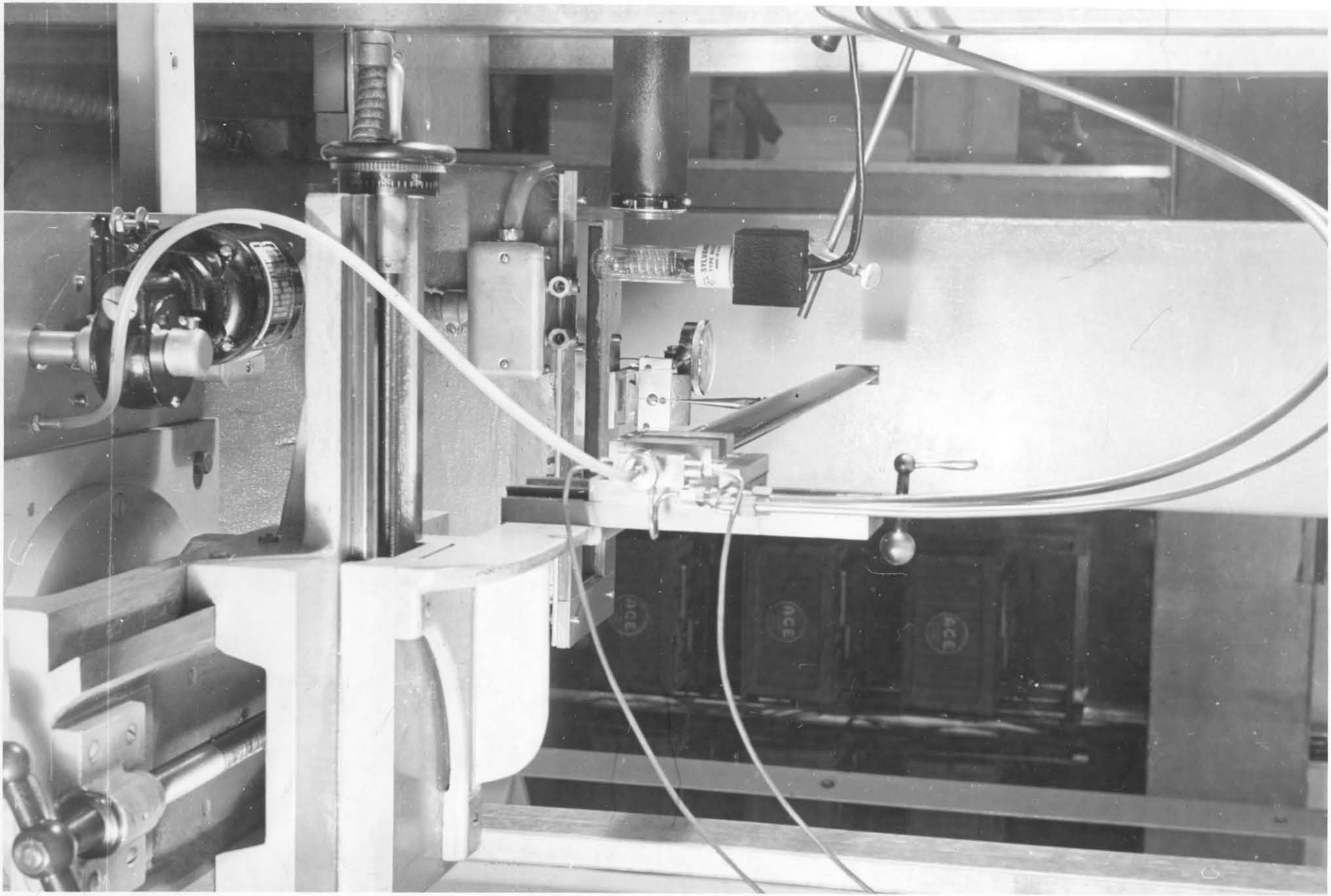

FIGURE 7 - WETTING DROPS

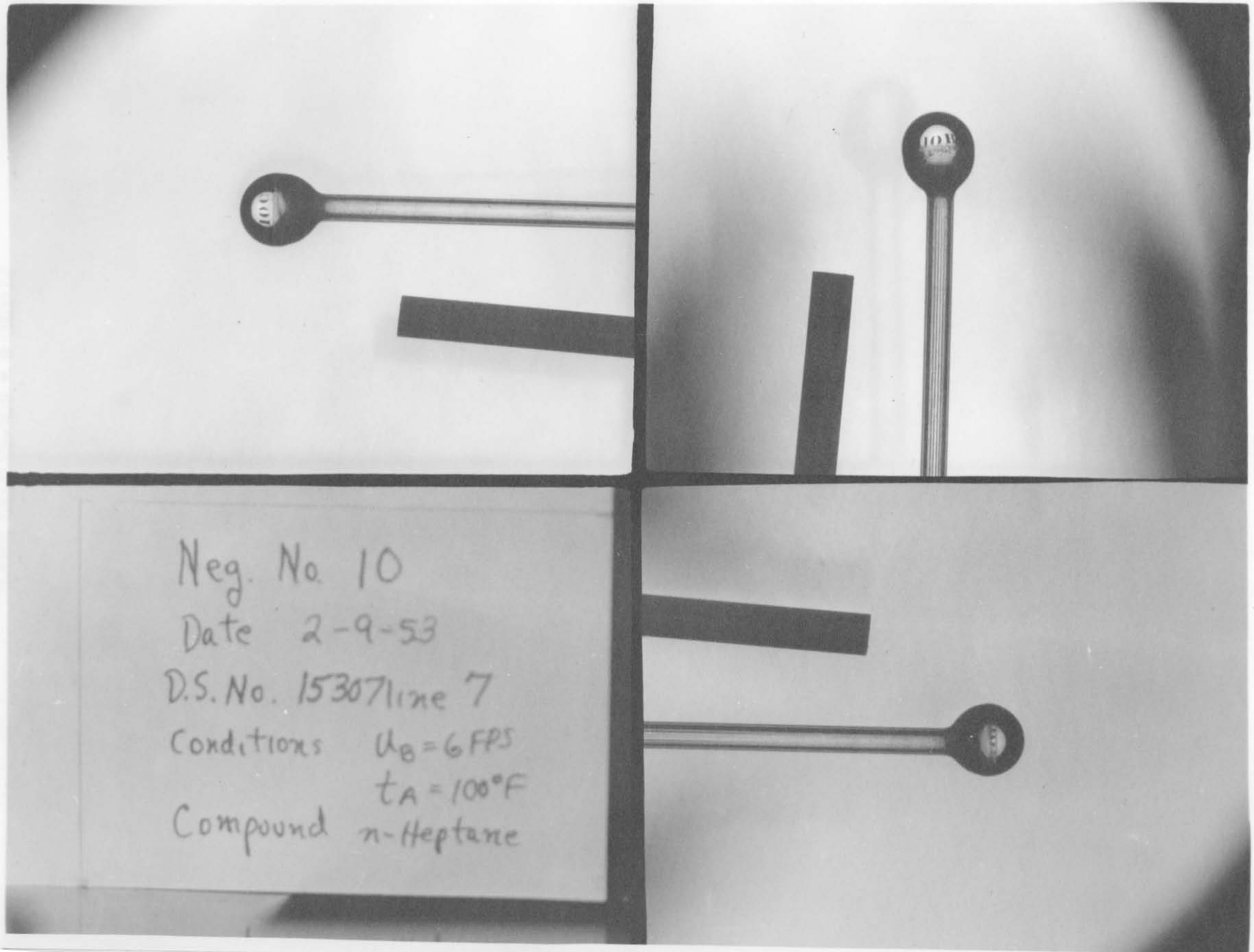
Neg. No. 10
Date 2-9-53
D.S. No. 15307 line 7
Conditions $U_B = 6$ FPS
$t_A = 100°F$
Compound n-Heptane

FIGURE 8 - NON-WETTING DROPS

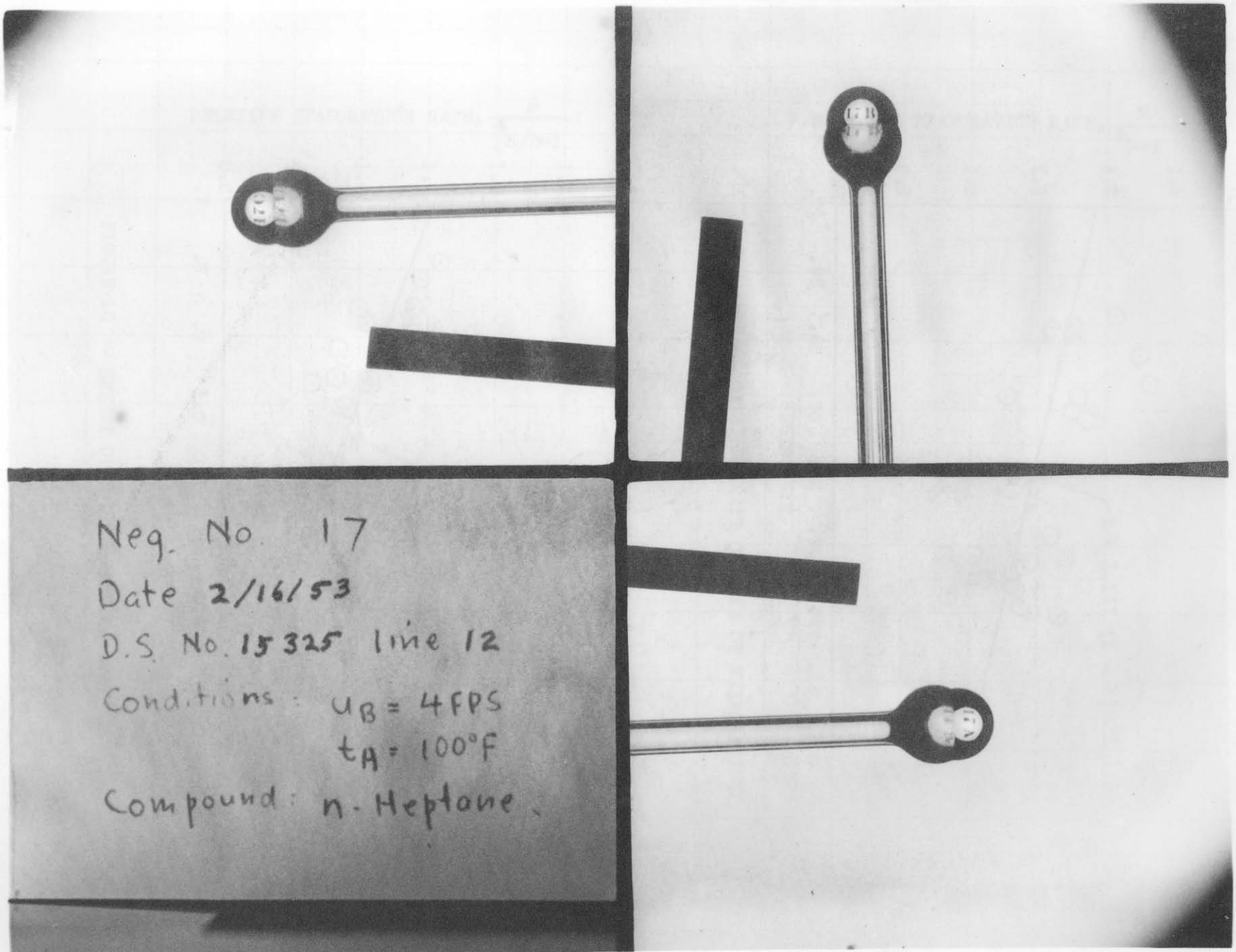
Neg. No. 17
Date 2/16/53
D.S. No. 15325 line 12
Conditions: u_B = 4 FPS
t_A = 100°F
Compound: n-Heptane.

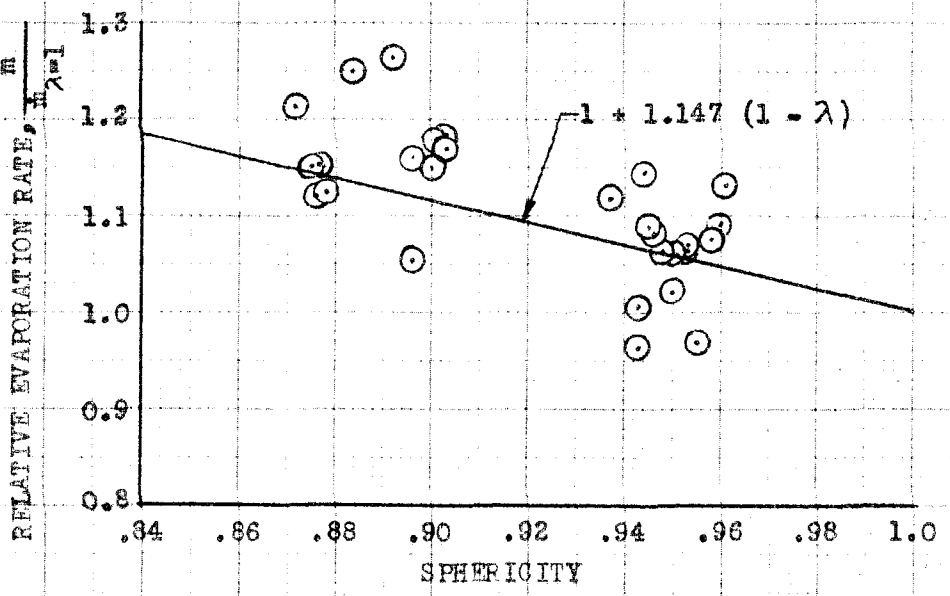

FIGURE 9 - EFFECT OF SPHERICITY ON RATE OF EVAPORATION

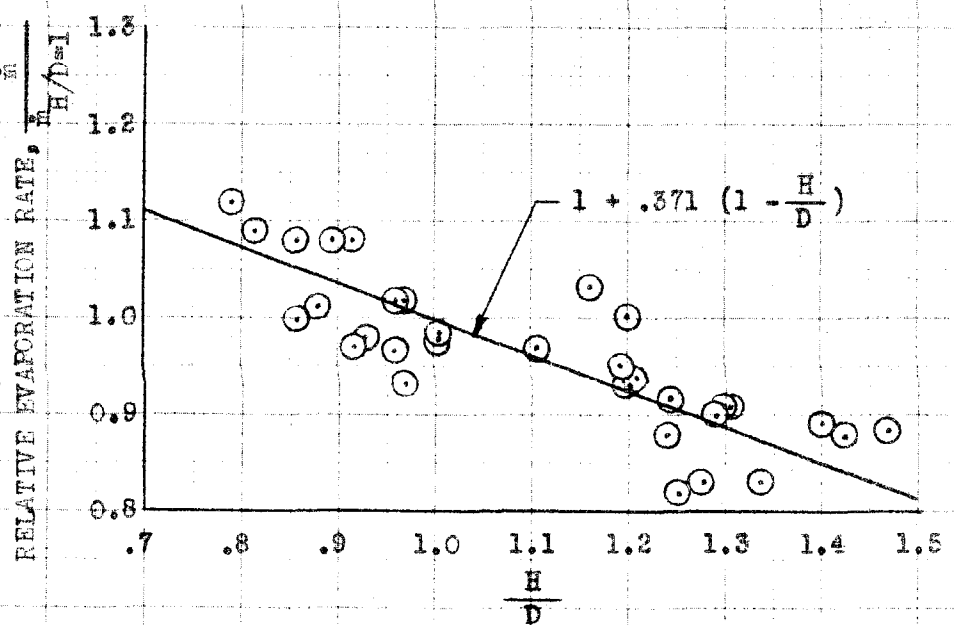

FIGURE 10 - EFFECT OF H/D ON RATE OF EVAPORATION

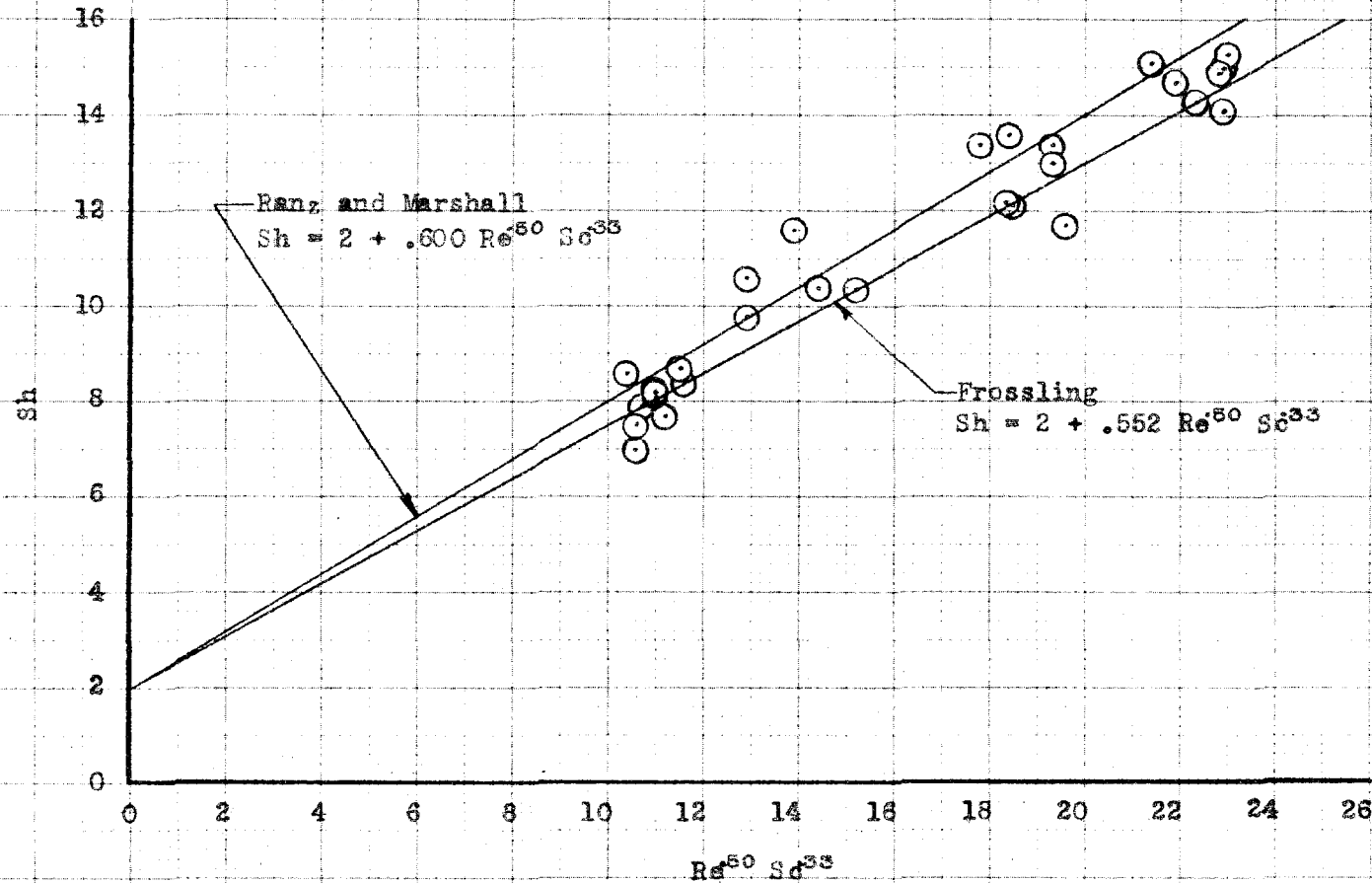

FIGURE 11 - CORRELATION OF MASS TRANSFER DATA

TABLE I EXPERIMENTAL DATA

DROP NUMBER	AIR VELOCITY FPS	MAXIMUM DIAMETER FT. 10^3	SURFACE AREA FT^2. 10^6	$\dot{m}$ LB/SEC 10^6	H/D	SPHERICITY	DROP TEMP. °F
24A	3.899	5.855	95.0	.15378	.878	.872	64.15
25A	3.937	5.359	69.3	.13220	.790	.887	64.33
26A	3.951	5.570	105.0	.15378	1.201	.961	62.33
27A	3.878	6.545	128.1	.18377	.968	.896	65.12
28A	3.884	5.306	70.7	.13220	.815	.884	66.07
30A	5.935	6.642	163.1	.24301	1.422	.960	61.88
31A	5.947	6.937	179.3	.25776	1.471	.944	61.92
32A	5.967	6.174	131.5	.21525	1.196	.958	61.63
32B	5.957	6.227	132.5	.21525	1.208	.953	61.63
32C	5.967	6.338	133.5	.21525	1.201	.951	61.63
34A	6.008	5.788	90.7	.18377	.857	.881	63.16
36A	6.022	6.177	106.1	.20362	.894	.892	62.73
37A	6.027	7.016	173.5	.24301	1.284	.955	63.27
38A	2.054	5.971	123.2	.13220	1.240	.950	63.60
39A	2.059	6.470	149.8	.15378	1.299	.946	62.65
39B	2.059	6.450	149.8	.15378	1.301	.945	62.65
39C	2.059	6.537	152.4	.15378	1.278	.948	62.65
40A	2.050	5.999	126.4	.13220	1.249	.943	65.14
41A	2.055	6.652	161.6	.15378	1.335	.943	63.70
42A	2.059	5.810	94.7	.13220	.914	.871	65.35
43A	2.060	6.536	130.8	.15378	1.006	.878	65.00
44A	2.044	7.159	195.0	.18377	1.402	.937	62.66
45A	2.044	6.143	108.9	.13220	.930	.875	65.32
46A	2.046	6.600	133.7	.15378	1.004	.876	64.78
47A	2.049	7.215	172.4	.18377	1.106	.876	64.35
48A	8.007	6.316	119.8	.24301	1.162	.884	62.26
49A	8.041	6.804	161.3	.27899	1.242	.953	62.22
50A	8.051	7.218	153.7	.27899	.859	.903	62.20
50B	8.051	7.078	148.8	.27899	.971	.899	62.20
50C	8.051	7.149	150.2	.27899	.962	.896	62.20
51A	8.072	6.526	121.1	.24301	.919	.901	62.64
55A	8.071	7.104	149.0	.27899	.961	.903	64.26

TABLE II - DERIVED DATA

DROP NUMBER	Re	Sc	$Re^{.5} Sc^{.33}$	Sh EXPERIMENTAL
24A	126.6	2.107	14.43	11.43
25A	116.8	2.111	13.94	12.12
26A	122.4	2.111	12.91	9.46
27A	140.4	2.104	15.18	10.69
28A	114.6	2.104	12.90	11.20
30A	227.7	2.087	19.29	11.47
31A	228.5	2.088	19.32	11.80
32A	204.0	2.090	18.26	11.89
32B	205.7	2.090	18.34	11.86
32C	207.4	2.090	18.50	11.83
34A	192.6	2.113	17.82	14.40
36A	206.0	2.117	18.43	14.64
37A	233.4	2.118	19.62	11.00
38A	68.0	2.106	10.57	7.20
39A	73.8	2.105	11.01	7.70
39B	73.5	2.105	10.99	7.70
39C	74.5	2.105	11.06	7.64
40A	67.9	2.101	10.55	6.17
41A	75.7	2.102	11.15	7.15
42A	66.2	2.102	10.43	9.57
43A	74.7	2.103	11.07	9.01
44A	81.0	2.105	11.52	7.89
45A	69.4	2.105	10.67	8.76
46A	74.9	2.108	11.10	8.98
47A	81.8	2.109	11.60	9.19
48A	279.7	2.105	21.43	16.04
49A	302.8	2.106	22.30	13.70
50A	321.7	2.106	22.99	16.10
50B	315.5	2.106	22.77	16.39
50C	318.7	2.106	22.88	16.50
51A	291.5	2.108	21.89	15.73
55A	316.9	2.117	22.86	15.44

APPENDIX

A set of four simultaneous, partial differential equations expressing the heat and mass transfer from drops can be developed from the boundary layer equations of Froessling (3) for a blunt-nosed solid of revolution. These can be expressed as follows in dimensionless quantities:

$$\left(\frac{1}{Pr\ Re}\right)\left\{\frac{1}{R^2}\ \frac{\partial}{\partial R}\left(R^2\ \frac{\partial T}{\partial R}\right) + \frac{1}{R^2 \sin\theta}\ \frac{\partial}{\partial R}\left(\sin\theta \frac{\partial T}{\partial \theta}\right)\right\} = V_r\ \frac{\partial T}{\partial R} + \frac{V_\theta}{R}\ \frac{\partial T}{\partial \theta} \quad (1)$$

(ENERGY BALANCE)

$$\left(\frac{1}{Sc\ Re\ P_f}\right)\left\{\frac{1}{R^2}\ \frac{\partial}{\partial R}\left(R^2\ \frac{\partial P_a}{\partial R}\right) + \frac{1}{R^2 \sin\theta}\ \frac{\partial}{\partial \theta}\left(\sin\theta\ \frac{P_a}{\theta}\right)\right\} = V_r\ \frac{\partial P_a}{\partial R} + \frac{V_e}{R}\ \frac{\partial P_a}{\partial \theta} \quad (2)$$

(MATERIAL BALANCE)

$$\frac{V_\theta}{R}\ \frac{\partial V_e}{\partial \theta} + V_r\ \frac{\partial V_e}{\partial R} = -\frac{1}{R}\ \frac{\partial P}{\partial \theta} + \frac{1}{Re}\ \frac{\partial^2 V_e}{\partial R^2} \quad (3)$$

(FORCE BALANCE)

$$\frac{1}{R}\ \frac{\partial}{\partial \theta}(R \sin\theta V_\theta) + \frac{\partial}{\partial R}(R \sin\theta V_r) = 0 \quad (4)$$

(EQUATION OF CONTINUITY)

with the boundary conditions

$$T = P_a = 0,\ V_e = V_r = 0,\ \text{at } R = 0.5$$

$$T = P_a = 1.0 \text{ at } R = \infty;\ V_e = v_r'/v_\infty,\ \text{at } R > \Delta/D$$

where Δ is the thickness of the boundary layer.

A general solution of this set of equations has not been made. Solutions have been found for special cases. The nature and extent of

the simplifying assumptions involved together with the complexity of the resulting expressions has limited the utility of these solutions. At zero velocity, it can be demonstrated from the foregoing equations that:

$$Nu = Sh = 2.0 \tag{5}$$

This indicates that the rate of change of surface area with respect to time for transient state evaporation of pure liquid drops is constant at zero velocity. This is in agreement with the experimental data of many investigators. For finite velocities, a number of solutions have been proposed, involving different assumptions. Most of these solutions have failed to agree with equation (5) at the limiting case of zero velocity. The complexity of these solutions in view of the simplifying assumptions involved in the derivation precludes their consideration here.

X NOMENCLATURE

A	Surface area of drop, ft^2
D	Maximum diameter of drop, ft
D_v	Mass diffusivity of n-heptane vapor in air, ft^2/sec
f_v	Fugacity of pure n-heptane, lb/ft^2
h_c	Convection heat transfer coefficient, Btu/sec ft^2 ^oF
H	Height of drop, ft
K_a	Thermal conductivity of air Btu/sec ft ^oF
K_v	Thermal conductivity of vapor, Btu/sec ft ^oF
M	Rate of evaporation from drop, lb/sec
Nu	Nusselt number = $\frac{D\, h_c}{K_a}$
P	Pressure, lb/ft^2
Pr	Prandtl number = $\frac{C_p\, \rho_a}{K_a}$
R	Dimensionless radial distance = $\frac{r}{D}$
Re	Reynolds number = $\frac{D\, U}{\nu}$
Sc	Schmidt number based on mass diffusivity of vapor = $\frac{P\nu}{D_v}$
Sh	Sherwood number, defined by equation (7)
t	Temperature, ^oF
T	Dimensionless temperature = $\frac{t - t_i}{t_o - t_i}$
U	Undisturbed air bulk velocity, ft/sec
V	Volume of drop, ft^3
V_r	Dimensionless radial velocity component
V_θ	Dimensionless angular velocity component

NOMENCLATURE (CONT.)

Greek Letters

α	Shape factor $= \frac{V}{A}$
Δ	Thickness of boundary layer
π	Total pressure
ν	Kinematic viscosity of air, ft^2/sec
θ	Angular coordinate measured from axis of drop
λ	Sphericity $= \frac{6\ V}{A\ D}$
ρ_a	Density of air, lb/ft^3

Subscripts

i	at the interface
o	in the main stream

XI REFERENCES

1. Langmuir, I., Phys. Rev., 12, 368-70 (1918)

2. Fuchs, N., Phys. Z. Sowjet, 6, 224-43 (1934), also available translated as N.A.C.A. Tech. Mem. 1160

3. Bradley, R. S., Evans, M. G., and Whytlaw-Gray, R. W., Proc. Roy. Soc. (London) A186, 368-90 (1946)

4. Froessling, M., Gerlands Beitr. Geophys., 52, 170-216 (1938)

5. Johnstone, H. F., Pigford, R. L., and Chapin, J. H., Trans. A. I. Ch. E., 37, 95-133 (1941)

6. Baer, D. H., Schlinger, W. G., Berry, V. J., and Sage, B. H., "Temperature Distribution in the Wake of a Heated Sphere" submitted to Jour. App. Mech.

7. Ingebo, R. D., Chem. Eng. Prog., 48, 403-8 (1952)

8. Ranz, W. E., and Marshall, W. R., Chem. Eng. Prog., 48, 141-6, 173-80 (1952)

9. El Wakil, M. M., Oydhara, O. A., Myers, P. S. N.A.C.A. Tech Note 3179 (1954)

10. Tung, L. H., and Drickamer, H. G., J. Chem. Phys., 20, 6-12 (1952)

11. Reamer, H. H., and Sage, B. H., "Method of Rate Measurement" Submitted to Rev. Sci. Inst.

12. Sato, K., Hsu, N. T., Reamer, H. H., and Sage, B. H., Am. Doc. Inst., Washington 25, D. C., Doc 4220 (1954)

13. Rossini, F. D., "Selected Values of the Lighter Hydrocarbons" Natl. Bur. Standards, Washington, D. C., November 1947

14. Page, F., Corcoran, W. H.,Schlinger, W. G., and Sage, B. H. Ind. Eng. Chem., 44, 419 (1952)

15. Hsu, N. T., Sato, K., and Sage, B. H., Ind. Eng. Chem. 46 870-6 (1954)

16. McAdams, W. H., "Heat Transmission" New York, McGraw-Hill Book Co., 2nd. Ed. (1942)